

Fast Semantic Segmentation on Video Using Motion Vector-Based Feature Interpolation

Samvit Jain and Joseph E. Gonzalez

University of California, Berkeley

Abstract. Models optimized for accuracy on challenging, dense prediction tasks such as semantic segmentation entail significant inference costs, and are prohibitively slow to run on each frame in a video. Since nearby video frames are spatially similar, however, there is substantial opportunity to reuse computation. Existing work has explored basic feature reuse and feature warping based on optical flow, but has encountered limits to the speedup attainable with these techniques. In this paper, we present a new, two part approach to accelerating inference on video. Firstly, we propose a fast feature propagation scheme that utilizes the block motion vector maps present in compressed video to cheaply propagate features from frame to frame. Secondly, we develop a novel feature estimation scheme, termed feature interpolation, that fuses features propagated from enclosing keyframes to render accurate feature estimates, even at sparse keyframe frequencies. We evaluate our system on the Cityscapes and CamVid datasets, comparing to both a frame-by-frame baseline and related work. We find that we are able to substantially accelerate segmentation on video, achieving twice the average inference speed as prior work at any target accuracy level.

Keywords: semantic segmentation · video · efficient inference

1 Introduction

Semantic segmentation, the task of assigning each pixel in an image to a semantic object class, is a problem of long-standing interest in computer vision. Since the first paper to suggest the use of fully convolutional networks to segment images [1], increasingly sophisticated architectures have been proposed, with the goal of segmenting more complex images, from larger, more realistic datasets, at higher and higher accuracy [2–5]. The result has been a ballooning in both model size and inference times, as the core feature networks, borrowed from image classification models, have grown in layer depth and parameter count, and as the cost of a forward pass through the widest convolutional layers, a function of the size and detail of the input images, has risen in step.

At the same time, a new target data format for semantic segmentation has emerged: video. The motivating use cases include both batch settings, where, for example, video is segmented in bulk to generate training data for other models (e.g. autonomous control systems), and streaming settings, where high-throughput video segmentation enables interactive analysis of live footage (e.g.

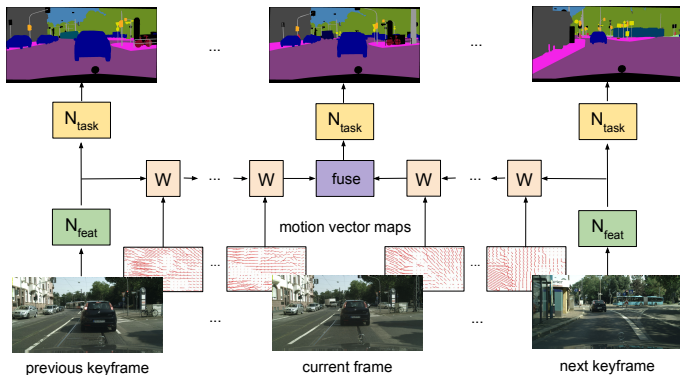


Fig. 1. Feature interpolation warps (W) and fuses the features of enclosing keyframes to generate accurate feature estimates for intermediate frames.

at surveillance sites). Video here consists of long sequences of images, shot at high frame rates (e.g. 30 frames per second) in complex environments (e.g. urban cityscapes) on modern, high-definition cameras (i.e. multi-megapixel). Segmenting individual frames at high accuracy still calls for the use of competitive image segmentation models, but the inference cost of these networks precludes their naive deployment on every frame in a multi-hour raw video stream.

A defining characteristic of realistic video is its high level of temporal continuity. Consecutive frames demonstrate significant spatial similarity, which suggests the potential to reuse computation across frames. Building on prior work, we exploit two observations: 1) higher-level features evolve more slowly than raw pixel content in video, and 2) feature computation tends to be much more expensive than task computation across a range of vision tasks (e.g. object detection, semantic segmentation) [6, 7]. Accordingly, we divide our semantic segmentation model into a deep feature network and a cheap, shallow task network [7]. We compute features only on designated keyframes, and propagate them to intermediate frames, by warping the feature maps with a frame-to-frame motion estimate. The task network is executed on all frames. Given that feature warping and task computation is much cheaper than feature extraction, a key parameter we aim to optimize is the interval between designated keyframes.

Here we make two key contributions to the effort to accelerate semantic segmentation on video. Firstly, noting the high level of data redundancy in video, we successfully utilize an artifact of compressed video, motion vector maps, to cheaply propagate features from frame to frame. Unlike other motion estimation techniques, which introduce extra computation on intermediate frames, motion vector maps are freely available in modern video formats, making for a simple, fast design. Secondly, we propose a novel feature estimation scheme that enables the features for a large fraction of the frames in a video to be inferred accurately and efficiently (see Fig. 1). The approach works as follows: when computing the segmentation for a keyframe, we also precompute the features for the *next*

designated keyframe. Features for all subsequent intermediate frames are then computed as a *fusion* of features warped forward from the last visited keyframe, and features warped backward from the incoming keyframe. This procedure thus implements an *interpolation* of the features of the two closest keyframes.

We evaluate our framework on the Cityscapes and CamVid datasets. Our baseline consists of running a state-of-the-art segmentation network, DeepLab [5], on every frame, a setup that achieves published accuracy [8], and a throughput of 1.3 frames per second (fps) on Cityscapes and 3.6 fps on CamVid. Our improvements come in two phases. Firstly, our use of motion vector maps for feature propagation allow us to cut inference time on intermediate frames by 50%, compared to approaches based on optical-flow, such as [7]. Secondly, our feature interpolation scheme enables us to operate at over twice the average inference speed as the fastest prior work, at any target level of accuracy. For example, if we are willing to tolerate no worse than 65 mIoU on our CamVid video stream, we are able to operate at a throughput of 20.1 fps, compared to the 8.0 fps achieved by the forward flow-based propagation from [7]. Overall, even when operating in high accuracy regimes (e.g. within 3% mIoU of the baseline), we are able to accelerate segmentation on video by a factor of 2-6x.

2 Related Work

Fast Video Inference. Prior work on accelerating video segmentation focuses on reducing the frequency of feature computations across frames. Schemes have been proposed to reuse cached feature computations from previous frames as is [6], and to propagate features forward from designated keyframes via warping with optical flow estimates (Zhu, et al., [7]). While the latter approach arguably supersedes the former by allowing feature maps to evolve across frames, it suffers from one key shortcoming, which this work seeks to address: features can be warped forward only as long as frame-to-frame changes consist primarily of internal displacements. Other forms of temporal evolution, such as the appearance of new objects, and simple perspective changes, such as camera pans, render past feature maps obsolete. In settings with complex dynamics, such as the urban environments captured in the Cityscapes dataset [9], or in footage with fast ego motion, features must be recomputed frequently, limiting the attainable speedup.

Recent work also explores alternatives to feature reuse. Mahasseni et al. use an LSTM network to select designated frames for full segmentation [10], and propagate final labels to other frames [11]. Zhu et al. augment their earlier work in [12], and look at feature estimate repair and adaptive keyframe scheduling. Using temporal information in video object detection and segmentation is also well-studied [13, 14], but not in the context of reducing inference costs.

Feature Fusion. Karpathy, et al. discuss various fusion schemes in the context of video classification [15], delineating early, late, and slow fusion approaches based on the stage at which information is merged. Fusion is implemented by

stacking input frames, and adding a fourth, temporal dimension to convolutional filters. Another body of work, starting with [16], studies spatial and temporal two-stream fusion for video action recognition [17–19]. Feichtenhofer, et al. look specifically at fusing feature maps in [17], and compare various spatial fusion techniques: sum fusion, max fusion, concatenation fusion, bilinear fusion, and convolutional fusion. They note both accuracy and parameter count-related tradeoffs, observations that broadly inform the choice of fusion strategies we consider. Recently, Jain et al. apply the two-stream model to video object segmentation, fusing appearance (i.e. frame-level) and motion (i.e. optical flow) streams to segment objects in weakly annotated videos [20]. In this paper, we do not further explore the two-stream model, and instead focus on applying basic feature fusion schemes, as in [17], to the problem of fast feature estimation.

Motion in Video. Fischer, et al. designed convolutional networks (FlowNet) to estimate optical flow [21, 22]. Their models are used to generate optical flow maps for feature warping in [7], and can be jointly trained with other components of the video segmentation network. Other commonly studied motion estimation schemes include point tracking [23] and scene flow estimation [24], but these demonstrate less applicability to the problem of warping 2D feature maps for semantic segmentation. In general, motion information has been used extensively to track and segment objects in videos [25–28].

Recent work by Wu, et al. proposes the idea of training directly on compressed video to improve both accuracy and performance on video action recognition [29]. Unlike [29], we use compressed video artifacts to infer motion for feature warping, not to reduce the size of input data. Moreover, our focus on pixel-level, dense prediction tasks, as opposed to video-level tasks [29, 30], places our work in a different space, one which requires rendering predictions for each uncompressed video frame and which calls in particular for inference speedups.

3 System Overview

3.1 Network architecture

For our semantic segmentation network, we adhere to the common practice of adapting a competitive image classification architecture (e.g. ResNet-101) into a fully convolutional network capable of outputting class predictions for each pixel in the input image (e.g. DeepLab) [1, 3, 5]. We identify two logical components in our final network: a *feature network*, which takes as input an image and outputs a high-resolution feature map, and a *task network*, which given a feature map, computes a class prediction for each pixel in the original image.

The feature network is obtained by eliminating the final, k -way classification layer in the chosen image classification architecture, and adjusting the feature stride to produce feature maps of the desired density. The task network is built by concatenating: 1) a 1×1 convolutional layer, with channel dimension $C + 1$, that predicts scores for each of C classes (plus background) in the target dataset,

2) a deconvolutional layer, which bilinearly upsamples the score maps to the resolution of the original image, and 3) a softmax layer, which converts scores to normalized probabilities for each pixel and each object class.

We divide our network into these two functional components for two reasons. Firstly, feature maps are transferable. As [6] observes, high-level feature maps evolve more slowly than raw pixels in a video. As a result, propagated features can serve as a good estimate for the features of proximate frames. Moreover, the fact that our feature outputs retain significant spatial structure means that we can often do better than mere copying, using estimates of frame-to-frame motion to instead *warp* feature maps forward. Secondly, feature computation is generally much more expensive than task computation for a range of vision tasks [7], an observation we formalize in Section 3.4. This, combined with the first idea, suggests the utility of only computing features on select frames, even if we must output segmentations for every frame in a video.

3.2 Motion vector maps

MPEG-compressed video consists of two logical components: reference frames, called I-frames, and delta frames, called P-frames. Reference frames are still RGB frames from the video, usually represented as spatially-compressed JPEG images. Delta frames, which introduce temporal compression to video, consist of two subcomponents: motion vector maps and residuals.

Motion vector maps, the artifact of interest in our current work, define a correspondence between pixels in the current frame and pixels in the previous frame. They are generated using the following simple *block-based motion estimation* procedure, a standard component of video compression algorithms [31]:

1. Divide the current frame into a non-overlapping grid of 16x16 pixel blocks.
2. For each block in the current frame, determine the “best matching” 16x16 block in the previous frame. A common matching metric is to minimize the mean squared error between the source block and the target block.
3. For each block in the current frame, represent the pixel offset to the best matching block in the previous frame as an (x, y) pair.

The resulting grid of (x, y) offsets forms the motion vector map for the current frame. For a frame of dimensions 16M x 16N, this grid has dimensions M x N.

3.3 Feature Propagation

Many cameras compress video by default as a means for efficient storage and transmission. The availability of a free form of motion estimation at inference time, the motion vector maps in MPEG-compressed video, suggests the following scheme for fast video segmentation (see Algorithm 1).

Choose a keyframe interval n , such that every n^{th} frame in the video is designated a keyframe, and all other frames are denoted intermediate frames. On keyframes, execute the feature network N_{feat} to obtain a feature map. Cache

these computed features (f_c), and then execute the task network N_{task} on the features to obtain the keyframe’s segmentation.

On intermediate frames, extract the motion vector map $mv[i]$ corresponding to the current frame index. Warp the cached feature map f_c one frame forward via bilinear interpolation with $-mv[i]$. (To warp forward, we apply the negation of the motion vector map.) Here we employ the differentiable, parameter-free warping operator [32] used also by [7]. Finally, execute N_{task} on the warped features to obtain the current segmentation, and update the cached features f_c .

Algorithm 1 Feature propagation

```

1: input: video frames  $\{I_i\}$ , motion vectors  $mv$ , keyframe interval  $n$ 
2: for frame  $I_i$  in  $\{I_i\}$  do
3:   if  $i \bmod n = 0$  then ▷ keyframe
4:      $f_i \leftarrow N_{feat}(I_i)$  ▷ keyframe features
5:      $S_i \leftarrow N_{task}(f_i)$ 
6:   else ▷ intermediate frame
7:      $f_i \leftarrow \text{WARP}(f_c, -mv[i])$  ▷ warp cached features
8:      $S_i \leftarrow N_{task}(f_i)$ 
9:   end if
10:   $f_c \leftarrow f_i$  ▷ cache features
11: end for
12: output: frame segmentations  $\{S_i\}$ 

```

Note that warping with a motion vector map has a natural analog in video decompression. A video decoder takes as input the previous frame and the current motion vector map, and outputs the current frame (modulo the residuals). Our warp operator takes the previous feature estimate and the current motion vector map, and outputs the current feature estimate.

3.4 Inference Runtime Analysis

Feature propagation is effective because it relegates feature extraction, the most expensive network component, to select keyframes. Of the three remaining operations performed on intermediate frames – motion estimation, feature warping, and task execution time – motion estimation with optical flow is the most expensive (see Fig. 2). By using motion vector maps, we eliminate this remaining bottleneck, accelerating inference times on intermediate frames from 116 ms per frame ($F + W + N_{task}$) to 54 ms per frame ($W + N_{task}$). For keyframe interval n , this translates to a speedup of 53% on $\frac{n-1}{n}$ of the video frames.

Note that for a chosen keyframe interval n , as inference on intermediate frames becomes cheaper, we approach a maximum attainable speedup factor of n over a frame-by-frame baseline that runs the full segmentation model on every frame. Having eliminated motion estimation, our achieved speedup factor now very closely trails the chosen keyframe interval. Significantly extending this interval, without compromising on accuracy, requires an entirely new approach to feature estimation, the subject of the next section.

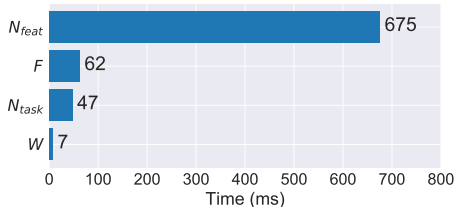


Fig. 2. A sample runtime breakdown. F is the optical flow net used in [7] for motion estimation. W is the warp operator. Models: DeepLab, ResNet-101. GPU: Tesla K80.

A potential objection here is that we have not accounted for the time required to extract motion vectors from raw video frames. Accordingly, we benchmarked the runtime of H.264 compression, finding that `ffmpeg` takes 2.78 seconds to compress 1,000 Cityscapes video frames, or 2.78 ms per frame. In contrast, computing optical flow on a pair of Cityscapes frames takes 62 ms (Fig. 2). We include this comparison for completeness; since compression is a default behavior, motion vector extraction time is not a true component of inference time.

3.5 Feature Interpolation

Given an input video stream and a segmentation network, we wish to compute the segmentation of every frame as efficiently as possible, while preserving accuracy. In a batch setting, we have access to the entire video, and want the segmentations for all the frames, as input to another model (e.g. an autonomous control system). In a streaming setting, we have access frames as they come in, but may be willing to tolerate a small delay of keyframe interval n frames ($\frac{n}{30}$ seconds or $33.3n$ milliseconds at 30 fps) before we output a segmentation, if that means we can keep pace with the stream and maintain high accuracy.

Granted the ability to look ahead n frames, we observe the following: a scheme that only propagates features forward from a designated keyframe can only capture the motion of objects present in that frame. Any new object that appears in the scene will be absent from the keyframe’s feature map, and from its warped representation as well. In highly dynamic settings, such as urban environments, this will force frequent recomputation of feature maps. This in turn severely caps the potential speedup, as average inference time is now primarily determined by the frequency at which the feature network is run (the keyframe interval).

Any intermediate frame in the video lies between two designated keyframes. Transient objects present in the intermediate frame are more likely to be present in the preceding *or* subsequent keyframe than in either individual keyframe alone. Feature fusion techniques are effective at preserving strong signals present in any one input feature map [17]. This suggests the following idea: estimate the features of intermediate frames as the fusion of the features of the enclosing keyframes, which represent bounds on the current scene.

Expanding on this idea, we propose the following algorithm (see **Alg. 2**). On any given keyframe, precompute the features for the *next* keyframe. On intermediate frames, warp the previous keyframe’s features, $N_{feat}(I_k)$, forward

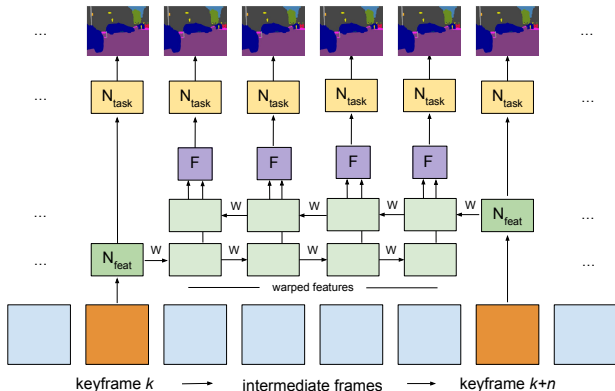


Fig. 3. In feature interpolation, features for intermediate frames are estimated as a fusion (F) of features warped (W) inward from enclosing keyframes.

to the current frame I_i using incremental forward motion estimates, $-mv[k : i]$. Warp the next keyframe’s features, $N_{feat}(I_{k+n})$, *backward* to the current frame using incremental backward motion estimates, $mv[k+n : i]$. Fuse the two feature maps using either a simple weighted average or a learned fusion operator, F . Then execute the task network N_{task} on the fused feature maps (see Fig. 3).

To eliminate redundant computation, on keyframes, we *precompute* forward and backward warped feature maps f^f, f^b corresponding to each subsequent intermediate frame, $\{I_{k+1}, \dots, I_{k+n-1}\}$. For keyframe interval n , this amounts to $n - 1$ forward warped feature maps and $n - 1$ backward warped feature maps.

We expect this scheme to outperform basic feature propagation for three reasons. Firstly, assuming fusion is beneficial, the fused feature maps will result in higher accuracy segmentations than using the forward or backward propagated feature maps alone. (In feature propagation, we only have access to the former.) Secondly, by propagating feature maps from both the previous and subsequent keyframes, we reduce the distance the closer keyframe’s features must be warped by a factor of two. Holding keyframe interval constant, in feature propagation, keyframe features are warped $\frac{n-1}{2}$ steps in expectation. In interpolation, the closer keyframe’s features are warped half as many steps in expectation. In other words, when features are warped in both directions, even if we were to just select the closer feature map (instead of fusing the two), we would have a better estimate of the current frame’s features. Lastly, since warping and fusion are significantly cheaper than other network components, interpolation adds little additional overhead. We validate all three observations in Section 4.

3.6 Feature Fusion

We consider several possible fusion operators, in particular: max fusion, average fusion, and convolutional fusion. Max fusion and average fusion are not learned, and are thus parameter-free. We implement max and average fusion by aligning the input feature maps $f^f, f^b \in R^{1 \times C \times h \times w}$ along the channel dimension, and

computing a maximum or average across each pixel in corresponding channels. We implement convolutional fusion by *stacking* the input feature maps along the channel dimension $[f^f, f^b]_C = f^s \in R^{1 \times 2C \times h \times w}$, and applying a bank of learned, 1x1 convolutional filters and biases that reduce the input channel dimensionality by a factor of two. In practice, we repurpose the first layer of the task network, which is itself a 1x1 conv layer, into our fusion layer, to avoid introducing a redundant 1x1 layer and adding to the total inference time.

Before applying the fusion operator at inference time, we weight the input feature maps with scalar values representing *feature relevance*. This transforms average fusion into a *weighted average fusion* and convolutional fusion into a *weighted convolutional fusion*, a scheme that works very effectively in practice. Specifically, we weight the two input feature maps f^f, f^b by scalars α and $1 - \alpha$, respectively, that correspond to propagation distance, penalizing features that have been warped farther from their keyframe. For keyframe interval n , and a frame at offsets p and $n - p$ from the previous and next keyframes, respectively, we set $\alpha = \frac{n-p}{n}$ and $1 - \alpha = \frac{p}{n}$. Thus, when p is small relative to n , we weight the previous keyframe’s features more heavily, and vice versa. As an example, when $n = 5$ and $p = 1$, we set $\alpha = \frac{4}{5}$ and $1 - \alpha = \frac{1}{5}$. To summarize, the features for intermediate frame I_i are computed as: $f_i = F(\frac{n-p}{n} f^f, \frac{p}{n} f^b)$, where $p = i \bmod n$. This weighting procedure is reflected in Algorithm 2.

Algorithm 2 Feature interpolation

```

1: input: video frames  $\{I_i\}$ , motion vectors mv, keyframe interval  $n$ 
2:  $W_f, W_b \leftarrow []$  ▷ forward, backward warped features
3: for frame  $I_i$  in  $\{I_i\}$  do
4:   if  $i \bmod n = 0$  then ▷ keyframe
5:      $k \leftarrow i$  ▷ keyframe index
6:      $f_k \leftarrow N_{feat}(I_k)$  ▷ curr keyframe features
7:      $S_k \leftarrow N_{task}(f_k)$ 
8:      $f_{k+n} \leftarrow N_{feat}(F_{k+n})$  ▷ next keyframe features
9:      $W_f \leftarrow \text{PROPAGATE}(f_k, n - 1, -\text{mv}[k + 1 : k + n])$ 
10:     $W_b \leftarrow \text{PROPAGATE}(f_{k+n}, n - 1, \text{mv}[k + n : k + 1])$ 
11:   else ▷ intermediate frame
12:      $p \leftarrow i \bmod n$  ▷ offset from prev keyframe
13:      $f_i \leftarrow F(\frac{n-p}{n} \cdot W_f[p], \frac{p}{n} \cdot W_b[n - p])$  ▷ fuse propagated features
14:      $S_i \leftarrow N_{task}(f_i)$ 
15:   end if
16: end for
17: output: frame segmentations  $\{S_i\}$ 

18: function PROPAGATE(features  $f$ , steps  $n$ , warp array  $g$ ) ▷ warp  $f$  for  $n$  steps
19:    $O \leftarrow [f]$ 
20:   for  $i = 1$  to  $n$  do
21:     append( $O$ , WARP( $O[i - 1], g[i]$ )) ▷ warp features one step
22:   end for
23:   return  $O$ 
24: end function

```

4 Experiments

4.1 Setup

Datasets. We train and evaluate our system on Cityscapes [9] and CamVid [33], two popular, large-scale datasets for complex urban scene understanding. Cityscapes includes 30-frame snippets of street scenes from 50 European cities, shot at a frame rate of 17 fps and at a resolution of 2048 by 1024 pixels. CamVid consists of over 10 minutes of 30 Hz footage captured at 960 by 720 pixels. Ground-truth labels are provided for the 20th frame in each Cityscapes **train** and **val** split snippet, and for every 30th frame in the CamVid dataset. On Cityscapes, we train on the **train** split and evaluate on the **val** split, following the example of previous work [3, 5, 7, 8]. On CamVid, we adopt the standard train-test split of Sturgess, et al. [34] We use the standard mean intersection-over-union (mIoU) metric to evaluate semantic segmentation accuracy, and measure throughput in frames per second (fps) to evaluate inference performance.

Architecture. For our segmentation network, we adopt the DeepLab architecture [5], which is widely considered state-of-the-art and a variant of which currently ranks at the top of the PASCAL VOC semantic segmentation performance challenge [35]. Beginning with a ResNet-101 model, we discard the last 1000-way classification layer, and reduce the feature stride from 32 to 16 to produce feature maps with the desired level of detail for semantic segmentation [7]. The 2048-dimensional outputs of this modified ResNet-101 base are used as inputs to our task network. As described earlier, our task network consists of: 1) a 1x1 convolutional layer, with channel dimension 20 or 12 (for the 19 and 11 output classes in Cityscapes and CamVid, respectively, plus background), 2) a deconvolutional layer which upsamples score predictions to 2048 by 1024 pixels, and 3) a softmax layer for outputting normalized probabilities.

Training. To train our single-frame DeepLab model, we initialize with weights from a ResNet-101 model that is pre-trained on ImageNet, and learn task-specific weights on the Cityscapes and CamVid **train** sets.

To train our video segmentation system, we start with the weights from this single-frame model. In each mini-batch, we sample at random a labeled image from the train set, and select a preceding frame to serve as the previous keyframe. For feature interpolation, we additionally select a subsequent keyframe. In each forward pass, we compute features on keyframes, warp the features using motion vector maps to the position of the sampled frame, and execute the task network on the warped (and potentially fused) features.

Since motion estimation with motion vector maps and feature warping are both parameter-free, training feature propagation consists simply of fine-tuning DeepLab weights on a more complex task. Note that training propagation based on optical flow, as in [7], does require learning and jointly fine-tuning the additional flow network weights [21]. Training feature interpolation with convolutional fusion involves learning weights for the fusion layer from scratch. We

implement a 1x1 convolutional fusion layer, which is applied to stacked feature maps, each with channel dimension 2048. This involves learning 2048 [1, 1, 4096] filters to render a fused feature map with the same dimensions as the inputs.

In all cases, we train with stochastic gradient descent on 4 Tesla K80 GPUs for 50 epochs, starting with a learning rate of 10^{-3} if learning any weights from scratch and 10^{-4} if fine-tuning.

Evaluation. To evaluate our video segmentation system on a sparsely annotated image dataset, we utilize the following setup. At inference time, we select an operational keyframe interval i , and iterate over the test examples, choosing keyframes such that the distance to the labeled frame rotates uniformly between 0 and $i - 1$. This sampling procedure simulates evaluation on a densely labeled video dataset, where $\frac{1}{i}$ frames fall at each keyframe offset between 0 and $i - 1$.

4.2 Results

Baseline. For our performance and accuracy baseline, we evaluate our full DeepLab model on every labeled frame in the Cityscapes and CamVid `test` splits. This frame-by-frame evaluation procedure forms the conventional approach to semantic segmentation on video. Our baseline model achieves accuracy 75.2 mIoU on Cityscapes, matching published results for the DeepLab architecture we used [8], and a throughput of 1.3 frames per second (fps). On CamVid, the baseline model achieves 68.6 mIoU at a throughput of 3.7 frames per second.

Propagation and Interpolation. In this section, we evaluate our two main contributions: 1) a fast feature propagation scheme based on MPEG motion vectors maps (**prop-mv**), and 2) feature interpolation, a new feature estimation scheme that couples propagation and feature fusion to render accurate segmentations at high keyframe intervals (**interp-mv**). We compare to the closest available existing work on the problem, a feature propagation scheme based on optical flow [7] (**prop-flow**).

We evaluate by comparing accuracy-runtime curves for the three approaches on Cityscapes and CamVid (see Figure 4). These curves are generated by plotting accuracy against throughput at each keyframe interval in Tables 1 and 3, which contain comprehensive results. We say a scheme that allows operation at higher accuracy at every throughput than another approach *strictly outperforms* it.

Firstly, we note that motion vector-based feature propagation (**prop-mv**) *outperforms* optical flow-based propagation (prop-flow) at all but the lowest throughputs. While motion vectors are slightly less accurate than optical flow in general, by cutting inference times by 53% on intermediate frames (Sec. 3.4), prop-mv allows operation at much lower keyframe intervals than optical flow to achieve the same inference speeds. This effect is pronounced enough to result in a much more favorable accuracy-throughput trade-off curve for prop-mv.

Secondly, we find that our feature interpolation scheme (**interp-mv**) *strictly outperforms* both feature propagation schemes. At every keyframe interval, interp-mv is more accurate than prop-flow and prop-mv; moreover, it operates at similar

Table 1. Accuracy and throughput on **Cityscapes** for three schemes: (1) optical-flow based feature propagation [7] (**prop-flow**), (2) motion vector-based feature propagation (**prop-mv**), and (3) motion vector-based feature *interpolation* (**interp-mv**).

Metric	Scheme	keyframe interval									
		1	2	3	4	5	6	7	8	9	10
mIoU, avg (%)	prop-flow	75.2	73.8	72.0	70.2	68.7	67.3	65.0	63.4	62.4	60.6
	prop-mv	75.2	73.1	71.3	69.4	68.2	67.3	65.0	64.0	63.2	61.7
	interp-mv	75.2	73.9	72.5	71.2	70.5	69.9	68.5	67.5	66.9	66.6
mIoU, min (%)	prop-flow	75.2	72.4	68.9	65.6	62.4	59.1	56.3	54.4	52.5	50.5
	prop-mv	75.2	71.3	67.7	64.8	62.4	60.1	58.5	56.9	55.0	53.7
	interp-mv	75.2	72.5	71.5	68.0	67.2	66.2	65.4	64.6	63.5	62.9
throughput (fps)	prop-flow	1.3	2.3	3.0	3.5	4.0	4.3	4.6	4.9	5.1	5.3
	prop-mv	1.3	2.5	3.4	4.3	5.0	5.6	6.2	6.7	7.1	7.6
	interp-mv	1.3	2.4	3.4	4.2	4.9	5.4	6.0	6.4	6.9	7.2

throughput to prop-mv. This translates to a consistent advantage over prop-mv, and an even larger advantage over prop-flow (see Fig. 4).

These trends are even more pronounced on the CamVid dataset (see Fig. 4b). Since CamVid consists of smaller images, shot at a higher frame rate, prop-mv and interp-mv achieve faster runtime speeds (up to 20+ fps) and lower accuracy degradation (less than 6%) than on Cityscapes. In particular, interp-mv actually registers a small *accuracy gain* over the baseline at keyframe intervals 2 and 3, utilizing multi-frame context to improve on the accuracy of the single-frame DeepLab model, in addition to achieving faster inference times.

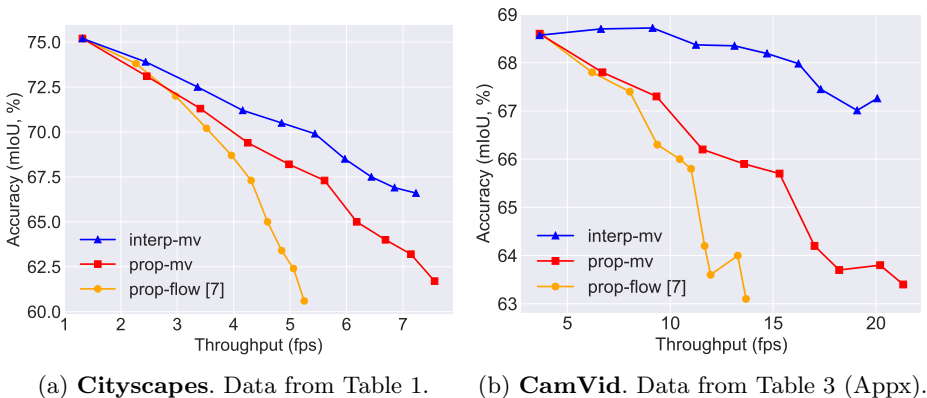


Fig. 4. Accuracy (**avg.**) vs. throughput for all schemes on Cityscapes and CamVid.

Metrics. We also note a distinction between two metrics: the standard *average* accuracy, the results for which are plotted in Fig. 4, and *minimum* accuracy,

which is a measure of the lowest frame-level accuracy an approach entails, i.e. accuracy on frames farthest away from keyframes (Appendix: Fig. 6). Minimum accuracy is the appropriate metric to consider when we wish to ensure that all frame segmentations are at least as accurate as some threshold value.

In particular, consider a batch processing setting in which the goal is to segment a video as efficiently as possible, at an accuracy target of no less than 65 mIoU on any frame, as calibrated at training time. As Table 1 demonstrates, at that accuracy threshold, feature interpolation enables operation at 6.0 fps on Cityscapes. This is significantly faster than achievable inference speeds with feature propagation alone, using either optical flow (3.5 fps) or motion vector maps (4.3 fps). In general, feature interpolation achieves almost twice the throughput as [7] on Cityscapes (*more* than twice on CamVid), at any target accuracy.

Baseline. We also compare to our frame-by-frame DeepLab baseline, which offers low throughput but high average accuracy. As Table 1 indicates, even at average accuracy about 70 mIoU on Cityscapes, a figure competitive with the best single-frame models [3, 5, 8], feature interpolation offers speedups of 2-4x over the baseline. On CamVid, the gains are even larger: at keyframe interval 10, interpolation achieves a 5.6x speedup over the baseline at just 1.3% lower mIoU. In fact, at keyframe interval 3, interpolation obtains a 2.5x speedup over the baseline, at slightly *higher* accuracy.

Delay. Finally, recall that to use feature interpolation, we must accept a delay of keyframe interval n frames, which corresponds to $\frac{n}{30}$ seconds at 30 fps. For example, at $n = 5$, interpolation introduces a delay of $\frac{5}{30}$ seconds, or 167 ms. By comparison, prop-flow [7] takes 250 ms to segment a frame at key interval 5, and interp-mv takes 200 ms. Thus, by lagging by less than 1 segmentation, we are able to segment 3.8x the frames per hour than the frame-by-frame model (5 fps vs. 1.3 fps). This is a suitable tradeoff in almost all batch settings (e.g. segmenting 1000s of hours of video to generate training data for a driverless vehicle; post-hoc surveillance video analysis), and in interactive applications such as video anomaly detection and film editing. Note that operating at a higher keyframe interval introduces a longer delay, but also enables much higher throughput.

Fig. 5 depicts a **qualitative comparison** of interpolation and prop-flow [7].

Feature Fusion. In this second set of experiments, we evaluate the accuracy gain achieved by feature fusion, and compare the various fusion strategies we considered. One goal of this analysis is to isolate the contribution of feature fusion to the success of our feature interpolation scheme.

As Table 2 demonstrates, utilizing any fusion strategy, including max, average, or conv fusion, results in higher accuracy segmentations than using either input feature map alone. This holds true even when one feature map is significantly stronger than the other (rows 2-4), and for both short distances and long distances to the keyframes. This observed additive effect suggests that feature fusion is highly effective at capturing signals that appear in only one input feature map, and in merging spatial information across time.

We also compared three fusion operators, max fusion, average fusion, and 1x1 conv fusion, to determine which result in the strongest segmentations. As Table

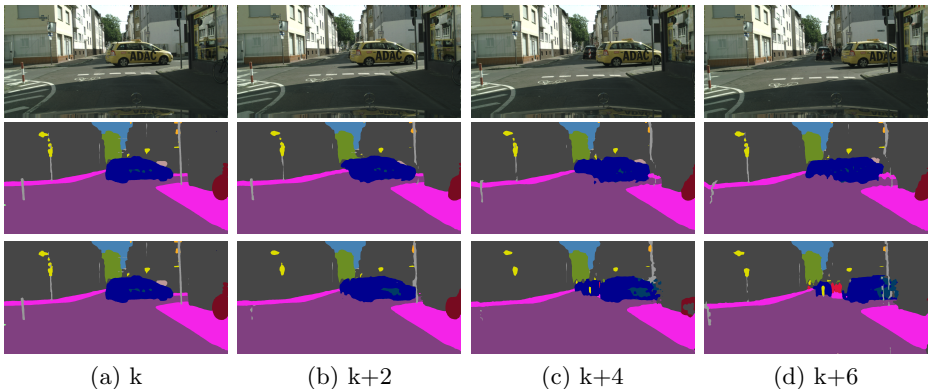


Fig. 5. Example segmentations at keyframe interval 7. Column $k + i$ corresponds to outputs i frames past the selected keyframe k . **First row:** input frames. **Second row:** prop-flow [7]. **Third row:** interp-mv (us). Note that, by $k + 6$, prop-flow has significantly warped the moving car, obscuring the people, vehicle, and street sign in the background (image center), while these entities remain clearly visible with interpolation. *Cityscapes*.

Table 2. An evaluation of feature fusion (Cityscapes). We report final accuracies for various keyframe placements. Forward and backward refer to the input feature maps.

Distance to keyframe(s)	forward mIoU	backward mIoU	max fusion mIoU	avg fusion mIoU	conv fusion mIoU
1	71.8	69.9	72.6	72.8	72.6
2	67.8	62.4	68.2	68.5	68.2
3	64.9	59.8	66.3	66.7	66.4
4	62.4	57.3	64.5	65.0	64.7

2 indicates, we found that while conv fusion generally outperformed max fusion, average fusion slightly outperformed conv fusion. We believe this is because average fusion is executed across corresponding feature channels, while the 1×1 conv, which operates on stacked feature channels, has access to no such mapping to start. This is an interesting finding we hope to investigate in future work.

5 Conclusion

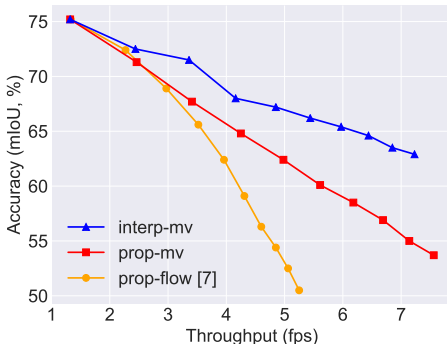
In this paper, we develop two main contributions: 1) a feature propagation scheme that uses motion vector maps to warp features from frame-to-frame cheaply and accurately, and 2) a new feature estimation scheme for video, termed feature interpolation, that utilizes feature propagation, frame information from the near future, and feature fusion, to produce accurate segmentations at high throughputs. We evaluate on the Cityscapes and CamVid datasets, and find that our schemes enable significant speedups, at any accuracy, over both a frame-by-frame baseline and prior work. Our methods are general, and represent an important advance in the effort to efficiently operate image models on video.

6 Appendix

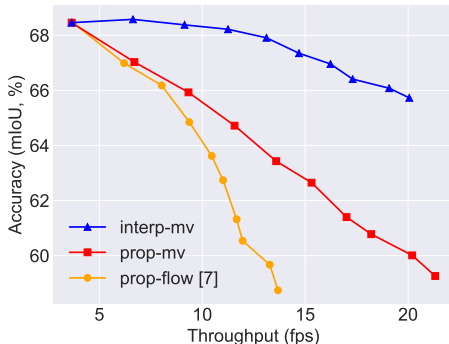
Results on the CamVid dataset (**Table 3**) and minimum accuracy vs. throughput plots for Cityscapes and CamVid (**Figure 6**).

Table 3. Accuracy and throughput on the **CamVid** dataset for the three schemes: prop-flow [7], prop-mv, and interp-mv.

Metric	Scheme	keyframe interval									
		1	2	3	4	5	6	7	8	9	10
mIoU, avg (%)	prop-flow	68.6	67.8	67.4	66.3	66.0	65.8	64.2	63.6	64.0	63.1
	prop-mv	68.6	67.8	67.3	66.2	65.9	65.7	64.2	63.7	63.8	63.4
	interp-mv	68.6	68.7	68.7	68.4	68.4	68.2	68.0	67.5	67.0	67.3
mIoU, min (%)	prop-flow	68.5	67.0	66.2	64.9	63.6	62.7	61.3	60.5	59.7	58.7
	prop-mv	68.5	67.0	65.9	64.7	63.4	62.7	61.4	60.8	60.0	59.3
	interp-mv	68.5	68.6	68.4	68.2	67.9	67.4	67.0	66.4	66.1	65.7
throughput (fps)	prop-flow	3.6	6.2	8.0	9.4	10.5	11.0	11.7	12.0	13.3	13.7
	prop-mv	3.6	6.7	9.3	11.6	13.6	15.3	17.0	18.2	20.2	21.3
	interp-mv	3.6	6.6	9.1	11.3	13.1	14.7	16.2	17.3	19.1	20.1



(a) **Cityscapes.** Data from Table 1.



(b) **CamVid.** Data from Table 3.

Fig. 6. Accuracy (**min.**) vs. throughput for all schemes on Cityscapes and CamVid.

On CamVid, interp-mv achieves *well over twice* the throughput as prop-flow, at any minimum accuracy threshold (see Fig. 6b). For example, at accuracy target 66 mIoU, interp-mv enables operation at 19.1 fps, compared to only 8.0 fps with prop-flow. At accuracy target 67 mIoU, interp-mv enables 16.2 fps, compared to 6.2 fps with prop-flow. This trend holds over the entire domain.

References

1. Long, J., Shelhamer, E., Darrell, T.: Fully convolutional networks for semantic segmentation. In: CVPR. (2015)
2. Badrinarayanan, V., Kendall, A., Cipolla, R.: Segnet: A deep convolutional encoder-decoder architecture for image segmentation. In: PAMI. (2017)
3. Yu, F., Koltun, V., Funkhouser, T.: Dilated residual networks. In: CVPR. (2017)
4. Lin, G., Milan, A., Shen, C., Reid, I.: Refinenet: Multi-path refinement networks for high-resolution semantic segmentation. In: CVPR. (2017)
5. Chen, L.C., Papandreou, G., Kokkinos, I., Murphy, K., Yuille, A.L.: Deeplab: Semantic image segmentation with deep convolutional nets, atrous convolution, and fully connected crfs. In: PAMI. (2017)
6. Shelhamer, E., Rakelly, K., Hoffman, J., Darrell, T.: Clockwork convnets for video semantic segmentation. In: Video Semantic Segmentation Workshop at ECCV. (2016)
7. Zhu, X., Xiong, Y., Dai, J., Yuan, L., Wei, Y.: Deep feature flow for video recognition. In: CVPR. (2017)
8. Dai, J., Qi, H., Xiong, Y., Li, Y., Zhang, G., Hu, H., Wei, Y.: Deformable convolutional networks. In: ICCV. (2017)
9. Cordts, M., Omran, M., Ramos, S., Rehfeld, T., Enzweiler, M., Benenson, R., Franke, U., Roth, S., Schiele, B.: The cityscapes dataset for semantic urban scene understanding. In: CVPR. (2016)
10. Mahasseni, B., Todorovic, S., Fern, A.: Budget-aware deep semantic video segmentation. In: CVPR. (2017)
11. Vijayanarasimhan, S., Grauman, K.: Active frame selection for label propagation in videos. In: ECCV. (2012)
12. Zhu, X., Dai, J., Yuan, L., Wei, Y.: Toward high performance video object detection. In: CVPR. (2018)
13. Kang, K., Li, H., Yan, J., Zeng, X., Yang, B., Xiao, T., Zhang, C., Wang, Z., Wang, R., Wang, X., Ouyang, W.: T-cnn: Tubelets with convolutional neural networks for object detection from videos. In: CVPR. (2016)
14. Kundu, A., Vineet, V., Koltun, V.: Feature space optimization for semantic video segmentation. In: CVPR. (2016)
15. Karpathy, A., Toderici, G., Shetty, S., Leung, T., Sukthankar, R., Fei-Fei, L.: Large-scale video classification with convolutional neural networks. In: CVPR. (2014)
16. Simonyan, K., Zisserman, A.: Two-stream convolutional networks for action recognition in videos. In: NIPS. (2014)
17. Feichtenhofer, C., Pinz, A., Zisserman, A.: Convolutional two-stream network fusion for video action recognition. In: CVPR. (2016)
18. Feichtenhofer, C., Pinz, A., Wildes, R.: Spatiotemporal residual networks for video action recognition. In: NIPS. (2016)
19. Feichtenhofer, C., Pinz, A., Wildes, R.P., Zisserman, A.: What have we learned from deep representations for action recognition? In: CVPR. (2018)
20. Jain, S.D., Xiong, B., Grauman, K.: Fusionseg: Learning to combine motion and appearance for fully automatic segmentation of generic objects in videos. In: CVPR. (2017)
21. Dosovitskiy, A., Fischer, P., Ilg, E., Häusser, P., Hazrbas, C., Golkov, V., v.d. Smagt, P., Cremers, D., Brox, T.: FlowNet: Learning optical flow with convolutional networks. In: ICCV. (2015)
22. Ilg, E., Mayer, N., Saikia, T., Keuper, M., Dosovitskiy, A., Brox, T.: FlowNet 2.0: Evolution of optical flow estimation with deep networks. In: CVPR. (2017)

23. Veenman, C.J., Reinders, M.J.T., Backer, E.: Motion tracking as a constrained optimization problem. *Pattern Recognition* **36** (2003) 2049–2067
24. Vedula, S., Baker, S., Rander, P., Collins, R., Kanade, T.: Three-dimensional scene flow. In: *ICCV*. (1999)
25. Papazoglou, A., Ferrari, V.: Fast object segmentation in unconstrained video. In: *ICCV*. (2013)
26. Fragkiadaki, K., Arbelaez, P., Felsen, P., Malik, J.: Learning to segment moving objects in videos. In: *CVPR*. (2015)
27. Nagaraja, N.S., Schmidt, F.R., Brox, T.: Video segmentation with just a few strokes. In: *CVPR*. (2015)
28. Tsai, Y.H., Yang, M.H., Black, M.J.: Video segmentation via object flow. In: *CVPR*. (2016)
29. Wu, C.Y., Zaheer, M., Hu, H., Manmatha, R., Smola, A.J., Krhenbhl, P.: Compressed video action recognition. In: *CVPR*. (2018)
30. Zhang, B., Wang, L., Wang, Z., Qiao, Y., Wang, H.: Real-time action recognition with enhanced motion vector cnns. In: *CVPR*. (2016)
31. Richardson, I.E.: *H.264 and MPEG-4 video compression: video coding for next-generation multimedia*. Wiley (2008)
32. Jaderberg, M., Simonyan, K., Zisserman, A., Kavukcuoglu, K.: Spatial transformer networks. In: *NIPS*. (2015)
33. Brostow, G.J., Fauqueur, J., Cipolla, R.: Semantic object classes in video: A high-definition ground truth database. *Pattern Recognition Letters* **30**(2) (2009) 8897
34. Sturgess, P., Alahari, K., Ladický, L., Torr, P.H.S.: Combining appearance and structure from motion features for road scene understanding. In: *BMVC*. (2009)
35. Aytar, Y.: Pascal voc challenge performance evaluation and download server. <http://host.robots.ox.ac.uk:8080/leaderboard> Accessed: 2018-03-06.